Domain formation in membranes with quenched protein obstacles: Lateral heterogeneity and the connection to universality classes

T. Fischer and R.L.C. Vink
Institute of Theoretical Physics, Georg-August-Universität Göttingen, Friedrich-Hund-Platz 1, D-37077 Göttingen, Germany

We show that lateral fluidity in membranes containing quenched protein obstacles belongs to the universality class of the two-dimensional random-field Ising model. The main feature of this class is the absence of a phase transition: there is no critical point, and macroscopic domain formation does not occur. Instead, there is only one phase. This phase is highly heterogeneous, with a structure consisting of micro-domains. The presence of quenched protein obstacles thus provides a mechanism to stabilize lipid rafts in equilibrium. Crucial for two-dimensional random-field Ising universality is that the obstacles are randomly distributed, and have a preferred affinity to one of the lipid species. When these conditions are not met, standard Ising or diluted Ising universality apply. In these cases, a critical point does exist, marking the onset toward macroscopic demixing.

PACS numbers: 87.16.dt, 64.60.-i, 61.20.Ja

I. INTRODUCTION

Membranes are two-dimensional (2D) fluid environments [1]. There is growing consensus that membrane lateral structure is heterogeneous, and characterized by domains of different size and composition [2–6]. Domain formation in biological membranes is important because it links to key processes in cells, such as signaling, endocytosis, and adhesion [7, 8], while in model membranes domain formation is relevant for applications, ranging from photolithographic patterning, spatial addressing, microcontact printing, and microfluidic patterning [9, 10]. To identify the factors that control domain formation, and to understand the underlying physical mechanisms, is therefore of practical importance.

In thermal equilibrium, a heterogeneous structure is difficult to comprehend, due to the large cost in line tension [2]. One instance where a heterogeneous structure does arise is near a critical point, as was demonstrated in free-floating giant unilamellar vesicles (GUVs) [11–13]. Near a critical point, the line tension vanishes; thermal motions then induce composition fluctuations over a wide range of length scales. An important concept in the theory of critical phenomena [13, 14] is universality: systems that belong to the same universality class undergo similar phase transitions, and yield the same set of critical exponents. For GUVs, the universality class was shown to be that of the 2D Ising model [11].

Since the universality class does not depend on the microscopic details of a system, it is tempting to speculate that 2D Ising universality, as observed in GUVs, is the generic class for membrane fluidity. The purpose of this paper is to show that, in less-idealized membranes (compared to GUVs), a different universality class comes into play, the reason being the presence of quenched obstacles. In living cells, proteins can bind to the underlying cytoskeleton [15]. This leads to a 2D fluid consisting of mobile particles (e.g. lipids) diffusing in a background of quenched (immobilized) protein obstacles. A similar situation arises in supported membranes, where surface friction may lead to particle immobilization [16]. Hence, to understand domain formation in membranes, it is important to keep in mind that an immobilized component may be present (in physical terms, such a system is called a quenched-annealed mixture [17]). Precisely this point was recognized by two recent simulation studies [18, 19] where domain formation in membranes with quenched protein obstacles was investigated. It was found that quenched obstacles lower the critical temperature [18, 19].

The aim of this paper is to relate the findings of Refs. 18 and 19 to universality classes. Our main message is that, in the presence of quenched obstacles, membrane fluidity belongs to the universality class of the 2D random-field Ising model (2D-RFIM). The 2D-RFIM is crucially different from the 2D Ising model because it does not feature a phase transition [20, 21]. Consequently, critical behavior and macroscopic phase separation do not occur, even in the limit of low obstacle concentration. This means that, irrespective of temperature and lipid composition, a membrane with quenched obstacles is always in the same thermodynamic phase. The structure of this phase is found to be heterogeneous, consisting of micro-domains. Hence, based on universality alone, one elegantly accounts for a heterogeneous *equilibrium* domain structure over a wide range of compositions and temperatures. In contrast, critical fluctuations persist only in a small region around the critical point.

The universality class of the 2D-RFIM applies when the protein obstacles display a preferred affinity to one of the lipid phases, and are randomly distributed. We believe this to be the typical situation in most membranes. When these conditions are not met, standard 2D Ising (as observed in GUVs) or diluted 2D Ising universality [22] will arise. However, deviations between the latter two classes are relatively small, in the sense that both feature a critical point, with similar critical exponents [23, 24].

II. MODEL AND METHODS

To illustrate these points, computer simulations of a 2D *off-lattice* mixture with quenched obstacles are performed. Since we focus on universality – which does not depend on microscopic details – it suffices to use a simple model. The protein obstacles are unit diameter disks, and are placed at the start of each simulation run on a $L \times L$ square with periodic boundaries, after which they remain quenched. The obstacles are mostly distributed randomly, although non-random choices will also be investigated. In line with recent simulations of membrane criticality [11–13, 25] a two-state model is used to describe the lipids, which diffuse through the environment of quenched obstacles. The model contains saturated (S) and unsaturated (U) lipids, both of which are disks having the same diameter as the obstacles. The sole interaction between lipids is a hard-core repulsion between unlike species, which is a minimum condition to induce phase separation [26]. In addition, the lipids interact with the quenched obstacles; these interactions will be specified later.

In ternary mixtures of saturated and unsaturated lipids with cholesterol, critical behavior occurs over a wide range of compositions and temperatures [27]. To induce critical behavior, one either varies the temperature at fixed composition, or one varies the composition at fixed temperature; both routes are experimentally accessible [28]. Since the interaction in our model is hard-core, we vary the lipid composition. This is done in grand-canonical Monte Carlo (MC) simulations, i.e. the respective fugacities z_S and z_U of saturated and unsaturated lipids are fixed, but the lipid number densities $\rho_X = N_X/L^2$ fluctuate, with N_X the number of lipids of species $X \in (U, S)$ in the system (see Ref. 29 for full details on the simulation method). The phase behavior is analyzed using the order parameter distribution (OPD) $P_{L,i}(\rho_U|z_U, z_S)$, defined as the probability to observe a state with unsaturated lipid density ρ_U. The OPD depends on the imposed fugacities, the system size L, as well as on the configuration i of quenched obstacles. Since universality applies to the thermodynamic limit $L \to \infty$, meaningful results require simulation data over a range of L, and the use of finite-size scaling (FSS) [30] to perform the extrapolation $L \to \infty$. In addition, in the presence of quenched obstacles, the shape of the OPD may fluctuate profoundly between obstacle configurations. It is therefore crucial to average simulation results over many $i = 1, \ldots, K$ different obstacle configurations.

III. RESULTS

A. pure lipid membrane: 2D Ising universality

We first consider a pure lipid membrane, i.e. without quenched obstacles (this qualitatively resembles a GUV).

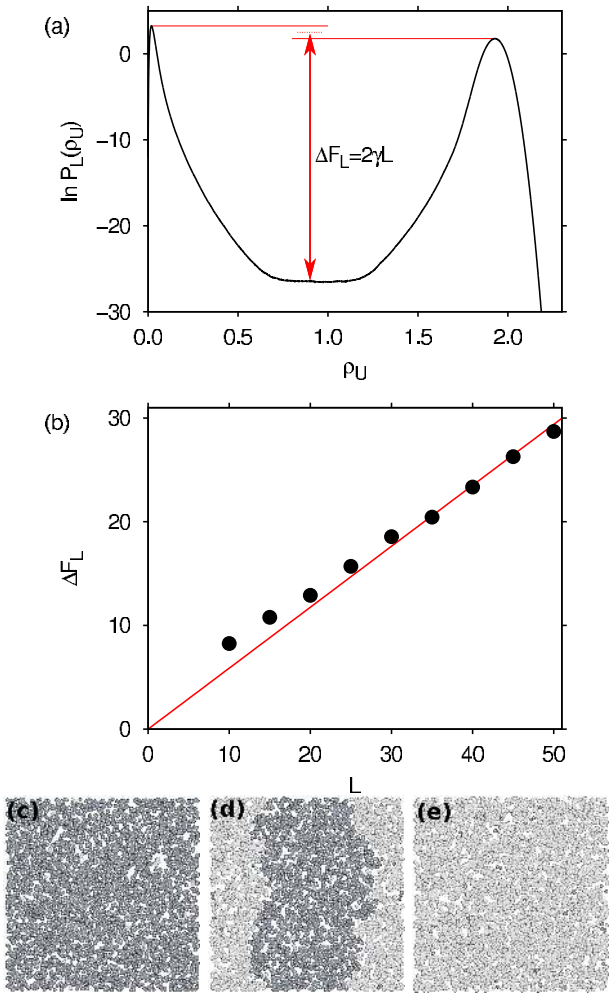

FIG. 1. Finite-size effects in a pure lipid membrane at fugacity $z_S = 2$ where the demixing transition is first-order. (a) The OPD for $L = 50$, and with z_U tuned according to Eq.(1). The distribution is distinctly bimodal. The vertical arrow marks the free energy barrier ΔF_L of interface formation. (b) The variation of ΔF_L with L. The linear increase confirms Eq.(2) of a genuine first-order transition; from the slope of the line the line tension can be extracted. The lower frames show snapshots of the membrane corresponding to the left peak of the OPD (c), the coexistence region between the peaks (d), and the right peak (e), where dark (light) particles represent saturated (unsaturated) lipids.

We thus simulate saturated and unsaturated lipids only, both species being mobile. The control parameters are the particle fugacities, z_S and z_U, and by appropriately tuning these parameters, phase transitions (provided they exist) can be induced. In some sense, the pure lipid membrane may be conceived as an *off-lattice* version of the 2D Ising model, with the role of temperature replaced by $1/z_S$, and that of the external field by $\ln z_U$. When z_S exceeds a critical value $z_S > z_{\rm cr}$, the transition is first-order and macroscopic phase separation is observed. When $z_S = z_{\rm cr}$, the transition becomes contin-

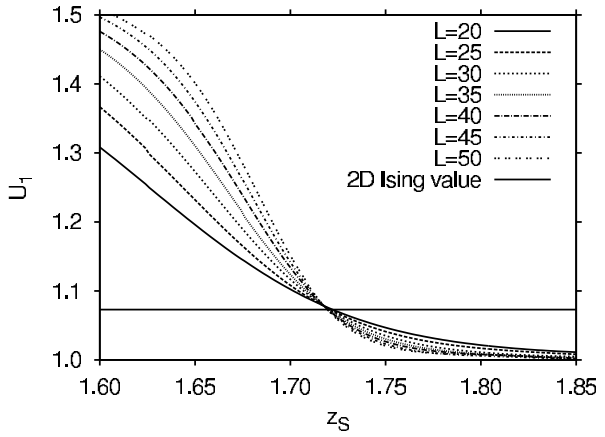

FIG. 2. Demonstration of the cumulant intersection method [31, 32] to locate the critical point in a membrane without quenched obstacles. Plotted is the cumulant U_1 versus the saturated lipid fugacity z_S for several system sizes L, and z_U tuned according to Eq.(1). At the critical point, the curves for different L intersect. The horizontal line marks $U_1^\star \approx 1.07$ of the 2D Ising universality class.

uous, and critical behavior is observed. When $z_S < z_{\rm cr}$, there is only one phase. At a phase transition, the scaling of the OPD with L assumes a characteristic form, from which the transition type can be determined. The observation of a transition also requires that z_U is chosen suitably. In what follows, for a given value of z_S, we tune z_U such that the derivative of the average saturated lipid density with respect to z_U is maximized

$$z_U : \frac{\partial \langle \rho_U \rangle}{\partial \ln z_U} \to \max, \tag{1}$$

as is commonly done in fluid simulations [33]. In the above, $\langle\cdot\rangle$ is a thermal average, i.e. an integral over the OPD: $\langle \rho_U \rangle = \int_0^\infty \rho_U \, P_L(\rho_U | z_U, z_S) \, d\rho_U$.

At a first-order transition the OPD is bimodal; see Fig. 1(a), where the natural logarithm of the distribution is shown (there is obviously no dependence on the obstacle configuration i in this case). Provided the bimodal shape persists in the thermodynamic limit $L \to \infty$, the peaks reflect stable phases. The peak on the right corresponds to a homogeneous phase rich in unsaturated lipids, and lean in saturated lipids (Fig. 1(c)). The left peak corresponds to a homogeneous phase of reversed composition (Fig. 1(e)), i.e. rich in saturated lipids, and thus resembles a lipid raft [5, 34, 35]. However, rafts are defined to be micro-domains, while the peaks in the OPD reflect macroscopic phases.

To verify that the bimodal shape survives in the thermodynamic limit, we consider the variation of the peak height ΔF_L with L (vertical arrow in Fig. 1(a)). We emphasize that ΔF_L is obtained from the natural logarithm of the OPD: it is defined as the average peak height, measured from the minimum "in-between" the peaks. When the simulation traverses the region between the peaks, phase coexistence is observed. Both phases then appear simultaneously. Exactly between the peaks, each phase occupies half the system: the phases then arrange in two slabs since this yields the shortest interface (Fig. 1(d)). Note that, due to periodic boundaries, two interfaces are present. If L is large enough, the interfaces do not interact with each other: the relative amount of the phases can then be varied over some range without any cost in free energy, which is the origin of the characteristic flat region between the peaks in the distribution of Fig. 1(a) [36]. Provided a flat region between the peaks is present, ΔF_L corresponds to the free energy cost of interface formation [37]. Since, in the slab arrangement, the total interface length $l_{\rm slab} = 2L$, it follows that

$$\Delta F_L = \gamma l_{\rm slab} = 2\gamma L, \tag{2}$$

with γ the line tension [37, 38]. At a first-order transition in 2D, we thus expect a linear increase of ΔF_L with system size. This is confirmed in Fig. 1(b), and from the slope of the line γ can be determined. Note that, for small L, corrections to Eq.(2) become important [39], as indicated by the systematic deviation of the simulation data away from a straight line for $L < 25$ or so.

Precisely at $z_S = z_{\rm cr}$, the first-order transition terminates in a critical point. The hallmark of criticality is scale invariance. This property can be exploited in FSS to extract $z_{\rm cr}$ from simulation data [31, 32]. To this end, one measures the Binder cumulant $U_1 = \langle m^2 \rangle / \langle |m| \rangle^2$, $m = \rho_U - \langle \rho_U \rangle$, which in the thermodynamic limit assumes three distinct values [30]. For $z_S > z_{\rm cr}$, i.e. where the transition is first-order and characterized by two-phase coexistence, the OPD is bimodal (Fig. 1(a)). The OPD may then be approximated by a superposition of two non-overlapping Gaussian peaks [40], which can be shown to yield $U_1 = 1$. For $z_S < z_{\rm cr}$, there is only one phase, with the OPD, consequently, featuring just a single peak. The peak is again Gaussian, for which $U_1 = \pi/2$. Precisely at the critical point, the OPD is bimodal, but the peaks overlap. As a result, the Binder cumulant at criticality assumes an "in-between" value $1 < U_1^\star < \pi/2$; scale invariance implies that $U_1^\star$ does not depend on L. Moreover, $U_1^\star$ is characteristic of the universality class, and for the 2D Ising model $U_1^\star \approx 1.07$.

In the thermodynamic limit, the Binder cumulant thus equals:

$$\lim_{L\to\infty} U_1 = \begin{cases} 1 & z_S > z_{\rm cr} \quad \text{(two-phase region)}, \\ U_1^\star & z_S = z_{\rm cr} \quad \text{(critical point)}, \\ \pi/2 & z_S < z_{\rm cr} \quad \text{(one-phase region)}. \end{cases} \tag{3}$$

This behavior is well-suited to obtain the critical fugacity $z_{\rm cr}$ from simulation data. To this end, one plots U_1 versus z_S for different system sizes (Fig. 2). At the critical point, the curves for different L intersect. From the intersection point we conclude that $z_{\rm cr} \approx 1.72$ for the membrane model without quenched obstacles [29]. Note also that U_1 at the intersection is close to the 2D Ising value (horizontal line). Hence, from the Binder cumulant alone, we

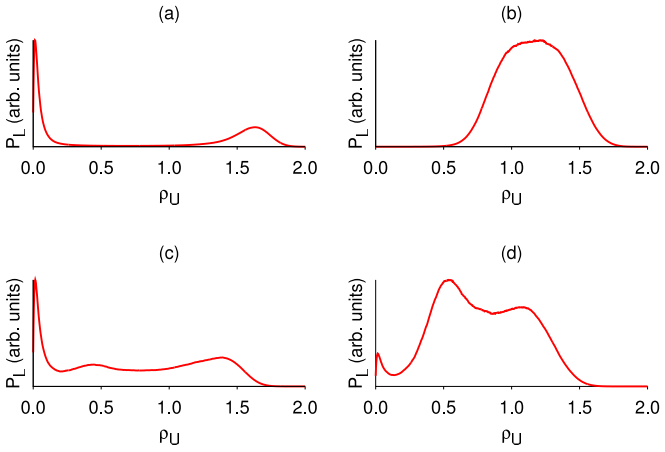

FIG. 3. Some example OPDs for a membrane with quenched obstacles, with the obstacles randomly distributed, and with a preferred affinity to saturated lipids. The key observation is that the distributions profoundly fluctuate between obstacle configurations, which illustrates the need for an extensive average over many obstacle configurations; data are shown for $L = 20$, $z_S = 1.92$, and z_U tuned according to Eq.(1).

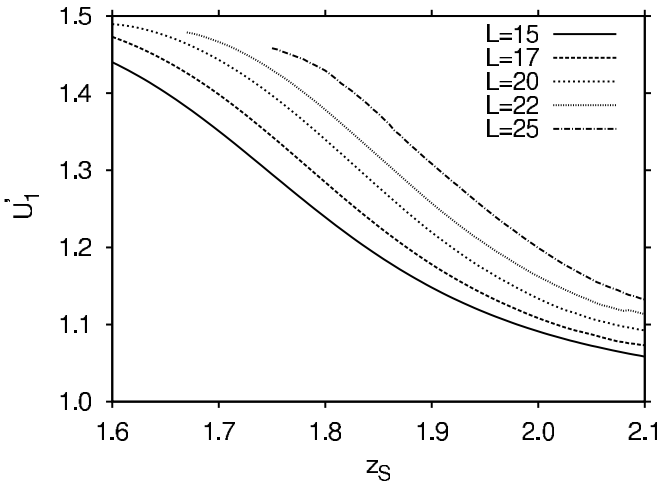

FIG. 4. Cumulant analysis of a membrane with quenched obstacles, with the obstacles randomly distributed, and with a preferred affinity to saturated lipids. Plotted is U_1' versus z_S for different L. An intersection point is not observed: this indicates the absence of a phase transition, which is consistent with the universality class of the 2D-RFIM.

prove the existence of a critical point, obtain an estimate of the critical fugacity, and confirm 2D Ising universality. The critical fugacity, as well as the total lipid density at criticality $\rho_{\rm cr} \approx 1.56$ (which was extracted from the critical OPD), are in good agreement with other studies [41]. Of course, since the pure membrane model is symmetric under the inversion of $U \leftrightarrow S$ lipids, it trivially follows that $\rho_S = \rho_U$ at the critical point.

B. random obstacles with preferred affinity: 2D random-field Ising universality

We now come to the main result of this paper, where we consider a membrane with quenched protein obstacles. The obstacles have a hard-core interaction with the unsaturated lipids, while saturated lipids may overlap freely with them. We thus impose a preferred affinity of the obstacles to lipid rafts, as, for example, GPI anchored proteins are known to do [34]. At the start of each simulation, we place Q obstacles randomly in the system, after which they remain quenched; Q is drawn from a Poisson distribution $P(Q) = (\lambda L^2)^Q e^{-\lambda L^2}/Q!$ with $\lambda = 0.03$ the average obstacle density. Next, saturated and unsaturated lipids are introduced, and the OPD is measured for the given configuration of quenched proteins. This procedure is repeated for many different obstacle configurations.

Since the proteins have a preferred affinity to one of the lipid species, and since they are randomly distributed, we expect 2D-RFIM universality. In particular: there should no longer be a phase transition. In Fig. 3, OPDs for a number of obstacle configurations are shown. The distributions were obtained for $z_S = 1.92$, which significantly exceeds $z_{\rm cr}$ of the membrane without quenched obstacles. We observe large shape variations. In (a) we see a bimodal distribution, which might be taken as evidence of a first-order transition. However, in (b) only a single peak is revealed, which rather reflects no transition at all. Finally, (c) and (d) show distributions with three peaks, suggesting a triple-point. We emphasize that all distributions in Fig. 3 were obtained at the same "inverse temperature" z_S and system size: only the obstacle configurations are different. Since the distributions show extreme shape variations between obstacle configurations, it is clear that meaningful results require an average over many obstacle configurations. One might object that the shape variations in Fig. 3 merely reflect a finite-size artifact, and that an average over obstacle configurations is not needed in larger systems. This, however, is a dangerous assumption because random-field systems are notoriously non-self-averaging [42, 43].

We thus use $K = 2000$ obstacle configurations in what follows, and perform a FSS analysis to obtain insight in the phase behavior in the thermodynamic limit. To this end, we consider the quenched-averaged cumulant $U_1' = [\langle m^2 \rangle]/[\langle |m| \rangle^2]$, with m and $\langle \cdot \rangle$ defined as before, and where $[\cdot]$ is an average over obstacle configurations. For each obstacle configuration i, the OPD is tuned according to Eq.(1) [44], which is then used to compute the thermal averages $\langle \cdot \rangle_i$; the latter are subsequently averaged over the obstacle configurations $[\langle \cdot \rangle] = (1/K) \sum_{i=1}^{K} \langle \cdot \rangle_i$. In Fig. 4, we plot U_1' versus z_S for different L. In contrast to Fig. 2, we cannot identify an intersection point. Instead, for a fixed value of z_S, the trend is that, by increasing L, the cumulant approaches the value of the one-phase region: $\lim_{L\to\infty} U_1' \to \pi/2$.

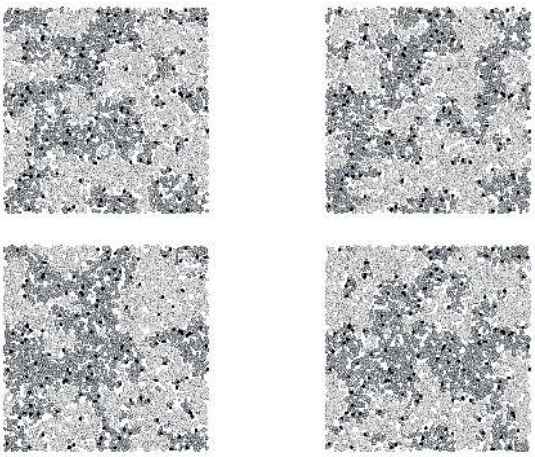

FIG. 5. Computer generated snapshots of domain formation in a membrane with quenched obstacles; $L = 60$, $\rho = 1.6$, and $\lambda = 0.04$ were used. The dark (light) regions correspond to saturated (unsaturated) lipids; dots mark the protein obstacles.

Hence, irrespective of z_S, in the thermodynamic limit $L \to \infty$ there is only one phase. In agreement with 2D-RFIM universality, a phase transition (above which coexistence between two macroscopic phases would occur) no longer takes place.

The reason macroscopic phase separation in the 2D-RFIM is prevented has a clear physical origin: in the presence of quenched obstacles the cost of line tension becomes negligible. To see this, consider a raft domain of radius R. The cost of line tension scales $\propto R^{d-1}$, with d the spatial dimension. However, the raft will also encompass a number of obstacles; the typical number of obstacles in the domain is $\propto R^d$ but with Poissonian fluctuations $\propto R^{d/2}$. Hence, it is favorable for the raft to seek out those regions in the membrane where there is an excess of obstacles. The cost of line tension is then compensated by the quenched obstacle excess, since $d = 2$ for membrane fluidity. Note that this reasoning is just the analogue of the Imry-Ma argument for random-field magnets [45].

Having shown that randomly distributed quenched proteins (with preferred affinity to one of the lipid species) prevent macroscopic phase separation, the structure of the remaining single-phase will now be analyzed. To this end, we perform canonical (fixed density) MC simulations using $\rho_S = \rho_U$ for different total densities $\rho := \rho_S + \rho_U$. In Fig. 5, we show a number of equilibrated snapshots at $\rho = 1.6$, $L = 60$, and using the same obstacle configuration each time; the obstacle concentration $\lambda = 0.04$. Note that $\rho = 1.6$ exceeds the critical density of the pure membrane and so, if we were to remove the obstacles, the snapshots would reveal macroscopic phase separation, and resemble Fig. 1(d). However, from the cumulant analysis of Fig. 3, it is clear that this does not happen in the presence of quenched proteins: there is no longer a critical point, and hence no longer a two-phase coexistence region. Instead, we see a structure consisting of micro-domains (by micro we mean that the typical domain size exceeds the typical distance between the obstacles but remains finite). We also see that the domain structure in each of the snapshots is different: this shows that thermal fluctuations are still present, and that the domains have a finite lifetime (which is important because rafts are believed to be short-lived). At first sight, the domains in the snapshots of Fig. 5 look deceivingly similar to critical fluctuations; see for example Fig. 1 of Ref. 11 where critical fluctuations in GUVs are shown. However, the domains in Fig. 5 are crucially different in two respects.

The first difference is that critical fluctuations are spatially indifferent: they can form at any location in the membrane with equal probability. In contrast, the domains that form in the presence of quenched obstacles are spatially selective: following the Imry-Ma argument, raft domains prefer to form at those locations in the membrane that feature an excess of obstacles. Of course, this spatial selection does not appear directly in single snapshots, but it becomes strikingly visible when we consider many snapshots and average over them. To demonstrate this explicitly, we use the same obstacle configuration of Fig. 5, and create a large number of equilibrated snapshots. For this set of snapshots, we construct an "ensemble-averaged" snapshot, simply by overlaying the individual snapshots. To this end, a grid consisting of unit square cells is placed over each individual snapshot. For each grid cell k, we sum over all snapshots, and count how often the cell contained a saturated lipid, or an unsaturated lipid; the counts are denoted $C_S(k)$ and $C_U(k)$, respectively. From these counts, we compute the canonical (or time) averaged lipid preference for each cell

$$A_k := \frac{C_U(k) - C_S(k)}{C_U(k) + C_S(k)}, \tag{4}$$

where a value $A_k = -1$ ($A_k = 1$) indicates a preference of cell k to saturated (unsaturated) lipids, while $A_k = 0$ indicates that a preferred affinity is absent.

In case of critical fluctuations, which are spatially indifferent, the structure revealed in individual snapshots gets completely "washed-out" in the averaged snapshot, since $A_k = 0$ for all cells in that case. In contrast, for the membrane with quenched obstacles, a clear structure in the averaged snapshot remains visible, which marks the regions in the membrane where rafts are most likely to be found. In Fig. 6, we show a number of averaged snapshots thus obtained, each one using the same obstacle configuration, but at different lipid densities ρ. The snapshots are color-coded, and the color reflects the value of A_k in the grid cell; dots mark the quenched protein obstacles. For all lipid densities considered, which even includes one density slightly below the critical density of the pure model, it is clear that lipid domains are spatially selective.

The second difference is that critical fluctuations van-

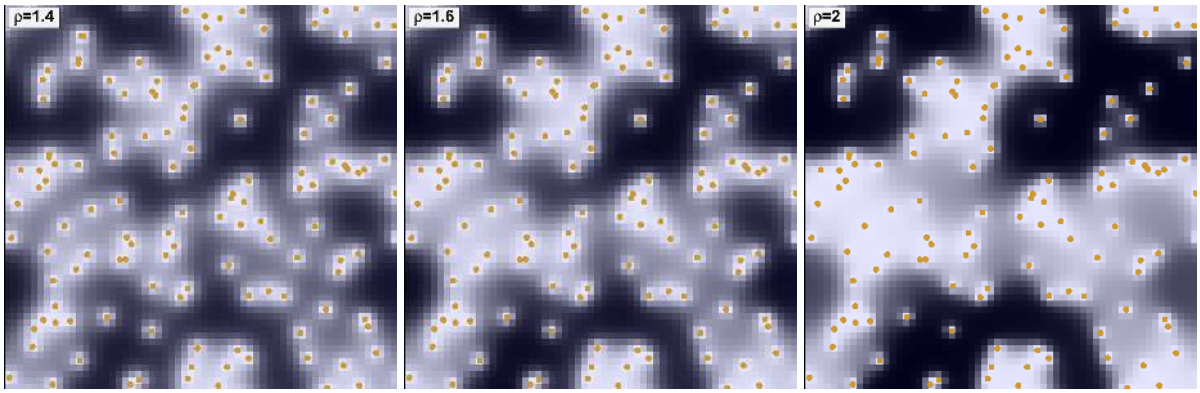

FIG. 6. Series of *ensemble-averaged* snapshots of a membrane with quenched protein obstacles, for three values of the lipid density ρ, using $L = 60$ and $\lambda = 0.04$. The images are color-coded, and the color reflects the local lipid preference A_k defined in Eq.(4), from $A_k = -1$ (brightest) to $A_k = 1$ (darkest); dots mark the protein obstacles. Note that the same obstacle configuration is used in all three cases; for a different analysis where also an average over obstacle configurations is performed, see Fig. 7. The images clearly show that the proteins create regions in the membrane where certain lipid species are preferred. In addition, the shape of these "preferred" regions is remarkably stable under variations in the lipid density.

ish above the critical density: the heterogeneous domain structure is then replaced by a coexistence between two (homogeneous) macro-domains. In contrast, the micro-domain structure in the membrane with quenched obstacles is stable upon variations in the total lipid density. The main effect of increasing ρ is a "freezing-out" of thermal fluctuations. At high density, the membrane becomes more spatially selective, and it becomes less likely to observe raft domains in regions where there is no obstacle excess. This is manifested in the averaged snapshots of Fig. 6 by a "sharpening" of the domain walls.

This effect can be made more precise when we convert each averaged snapshot of Fig. 6 into a one-dimensional histogram of A_k values, and to subsequently average these histograms over a number of obstacle configurations. Of course, in this way we loose the spatial correlations, but it allows us to verify that the spatial selectivity shown in Fig. 6 is a generic feature, and not just an artifact of the particular obstacle configuration that was used. In Fig. 7, we show histograms of A_k values thus obtained, which were averaged over 20 different protein configurations, and again for three lipid densities ρ. Note that the sharp peak at $A_k = -1$, in particular for the $\rho = 1.4$ histogram, is partially due to grid cells containing an obstacle. By increasing ρ, the extreme values $A_k \sim \pm 1$ become more likely, which confirms that the preference for certain lipids at certain locations in the membrane becomes more pronounced. The histograms also reveal another important point: even at density $\rho = 1.4$, i.e. below the critical density of the pure model, the membrane with quenched proteins is already spatially selective, since no peak around $A_k = 0$ is visible.

To summarize: in the presence of quenched proteins, randomly distributed, and with a preferred affinity to one of the lipid species, there is no sign of a phase transition leading to two-phase coexistence, nor of a critical point.

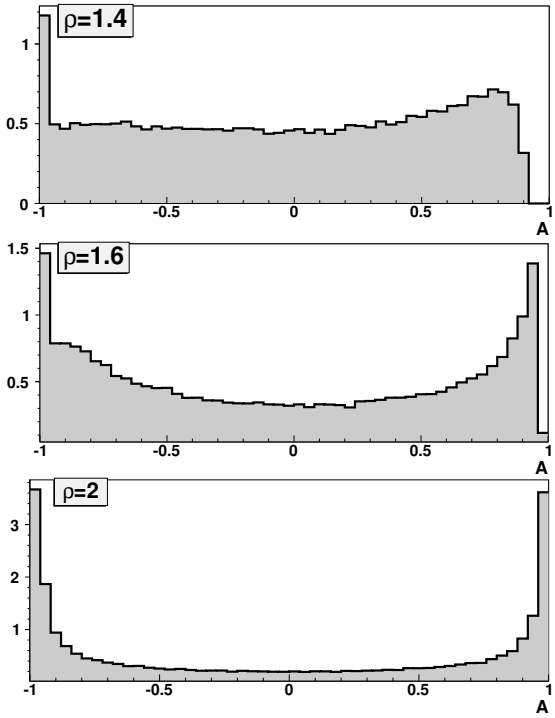

FIG. 7. Histograms of observed A_k values for different values of the lipid density ρ collected over 20 obstacle configurations.

Instead of the lipids forming two macroscopic domains, micro-domains are observed. These micro-domains are dynamic, but they do not diffuse over the membrane randomly: they are most likely to be found in regions of the membrane featuring an excess of obstacles. In some sense, the quenched protein obstacles provide a scaffolding (channels) extending over the membrane for raft domains.

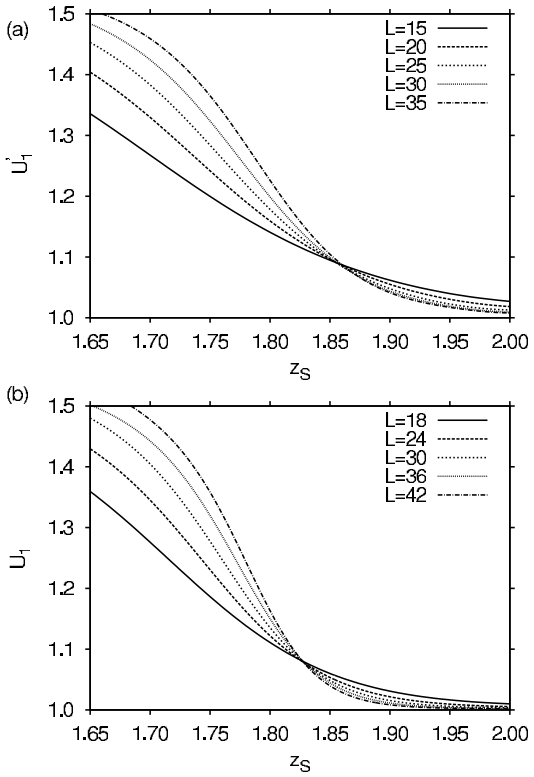

FIG. 8. (a) Cumulant analysis of a membrane with quenched protein obstacles that are randomly distributed, but without a preferred affinity to one of the lipid species. The curves of U_1' versus z_S for different L reveal an intersection point, consistent with the occurrence of a phase transition. (b) The same analysis as above, but for protein obstacles with a preferred affinity to saturated lipids placed on a regular grid. Curves of U_1 versus z_S for different L intersect, consistent with the occurrence of a phase transition.

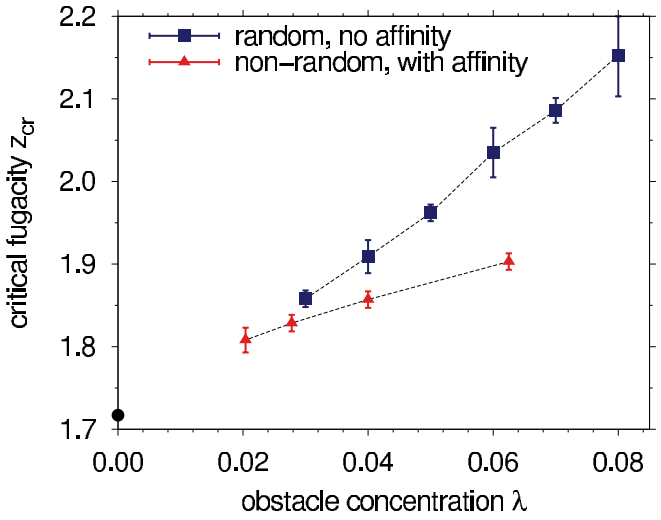

FIG. 9. Variation of the critical fugacity $z_{\rm cr}$ with obstacle concentration λ for a membrane with neutral obstacles that are randomly distributed (squares), and for a membrane with obstacles featuring a preferred affinity to saturated lipids, but placed on a regular grid (triangles). The dot at $\lambda = 0$ marks $z_{\rm cr}$ of the pure membrane; lines serve to guide the eye.

C. random obstacles without preferred affinity : diluted 2D Ising universality

We now consider a membrane with protein obstacles that do not have a preferred affinity to one of the lipid species, i.e. are neutral, but remain randomly distributed. To this end, we use the rule that neither lipid species may overlap with the obstacles; the average obstacle concentration $\lambda = 0.03$, again drawn from a Poisson distribution. The Imry-Ma argument does not apply in this case, and we indeed find a radical departure from 2D-RFIM universality. Instead, the scenario of Fig. 1 is recovered, and a genuine phase transition is observed. In Fig. 8(a), we show the variation of the cumulant U_1' with z_S, for different system sizes. An intersection point is revealed, proving the existence of a critical point, and for the critical fugacity we obtain $z_{\rm cr} \approx 1.86$. Since there is no longer a preferred affinity, the protein obstacles cannot compensate the cost of line tension. The membrane thus seeks to minimize the amount of interface, implying the formation of macroscopic domains when $z_S > z_{\rm cr}$. Hence, in the presence of neutral obstacles, the only instance where a heterogeneous domain structure *in equilibrium* can arise is near the critical point. The corresponding critical fluctuations will be qualitatively similar to those of the pure membrane, i.e. they are dynamic, and spatially indifferent (since the membrane with neutral obstacles remains symmetric under inversion of $U \leftrightarrow S$ lipids, it trivially follows that the averaged lipid preference $A_k = 0$).

We emphasize that the case of neutral obstacles closely resembles the membrane simulations of Ref. 18. In that work, the 2D Ising model is studied, but with a fraction of randomly chosen lattice sites "turned-off" to represent quenched protein obstacles. The key point is that this kind of dilution disorder does not break the up/down symmetry of the Ising model, just as the neutral obstacles in our model do not break the $U \leftrightarrow S$ lipid symmetry. Consequently, both models belong to the same universality class, namely the one of the 2D diluted Ising model. For this universality class, there is no doubt that a phase transition exists [22], provided the dilution remains below the limit where the lattice becomes disjoint. Indeed, an analysis of the Binder cumulant in Ref. 18 also reveals an intersection point, in agreement with our Fig. 8(a). A second hallmark of diluted Ising universality is a pronounced decrease of the critical temperature with increasing obstacle concentration. This was strikingly confirmed in Ref. 18, and our data reveal the same trend (Fig. 9). Note that z_S in our model plays the role of inverse temperature, so $z_{\rm cr}$ increases with the obstacle concentration. Finally, we point out that the extreme fluctuations of the OPD between obstacle configurations that characterize the random-field case (Fig. 3) do not

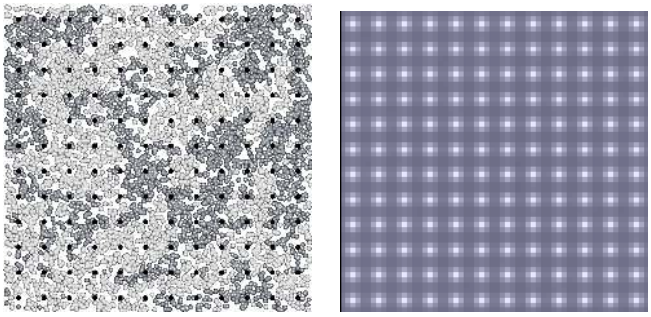

FIG. 10. Structure analysis of a membrane containing quenched protein obstacles; the obstacles have a preferred affinity to saturated lipids, and are placed on a grid with a lattice constant of five particle diameters. The left frame shows a single snapshot taken at densities slightly below the critical values $\rho_{U,\mathrm{cr}} \approx 0.82$ and $\rho_{S,\mathrm{cr}} \approx 0.90$ (due to the preferred affinity, it does not hold that $\rho_{U,\mathrm{cr}} = \rho_{S,\mathrm{cr}}$). The right frame shows the corresponding *ensemble-averaged* snapshot. The main message is that the structure seen on the left is completely washed out. All that remains is a locally enhanced saturated lipid density around each obstacle.

occur in the diluted Ising model.

D. non-random obstacles with preferred affinity : 2D Ising universality

Finally, we consider a membrane containing quenched proteins with a preferred affinity to saturated lipids, but placed non-randomly, namely on the sites of a square lattice. The lattice constant is six particle diameters, corresponding to an obstacle density $\lambda \approx 0.03$. In this case, the Imry-Ma argument does not apply either, because local (Poissonian) fluctuations in the obstacle density do not occur; note also that a disorder average $[\cdot]$ is not needed either. In Fig. 8(b), we show the cumulant U_1 versus z_S for different L. We observe an intersection point, which proves the existence of a critical point, and for the critical fugacity $z_{\mathrm{cr}} \approx 1.83$ is obtained. Hence, the scenario of Fig. 1 is recovered, with macroscopic phase separation taking place when $z_S > z_{\mathrm{cr}}$. By placing the protein obstacles at regular locations, the universality class remains that of the standard 2D Ising model. The only effect the proteins induce is confinement of the fluid, leading to a decrease of the critical temperature. Indeed, if we repeat the analysis using different lattice constants for the obstacle grid, we systematically find that z_{cr} increases with obstacle concentration (Fig. 9).

Hence, with the obstacles placed on a grid, an equilibrium heterogeneous domain structure only survives at the critical point. A typical snapshot obtained near criticality is given in the left frame of Fig. 10, where now lattice constant five was used. Even though the obstacles have a preferred affinity to saturated lipids, this is not sufficient to stabilize a structure consisting of micro-domains. This becomes clear when one constructs the corresponding *ensemble-averaged* snapshot (conform Fig. 6) which we show in the right frame of Fig. 10. In the averaged snapshot, the structure seen in the single snapshot is completely washed out. Of course, due to the preferred affinity to saturated lipids, there is a layer of enhanced saturated lipid density around each obstacle, but this layer is restricted to a single obstacle. These layers do not extend to other obstacles to form micro-domains (one might regard them as nano-domains instead). In contrast, the micro-domains in Fig. 6 extend over numerous protein obstacles.

E. Conclusion

Inspired by recent simulations of membranes with quenched protein obstacles [18, 19], additional simulations were performed with the aim to relate domain formation in these systems to universality classes. The main message is that, while a membrane without quenched obstacles is in the universality class of the 2D Ising model [11], the introduction of obstacles will in most practical situations induce a change to 2D random-field Ising universality. The consequences are drastic: the phase transition of the pure membrane without obstacles is destroyed, macroscopic phase separation no longer occurs, and only a single phase survives consisting of micro-domains. These micro-domains prefer to form at special regions in the membrane, and this preference becomes more pronounced with increasing lipid density. It would be of great interest to see whether transport of particles happens along the same regions; in that case, quenched proteins truly provide a structure of channels along which membrane constituents are laterally transported.

We have also considered two somewhat "artificial" cases, whereby the quenched obstacles are neutral, or placed regularly on a grid. In these cases, a normal critical phase transition is observed, above which macroscopic phase separation takes place. These predictions are presumably less relevant for biological cells, but they could be verified in experiments on model membranes (using, for example, an appropriately patterned surface [46]). We write *presumably* above because the spectrin cytoskeleton network in red blood cells does, in fact, form a regular lattice structure [47].

On a more fundamental level, the connection between a fluid with quenched obstacles (with preferred affinity) and random-fields dates back to de Gennes [48], but has been notoriously difficult to verify experimentally (see Ref. 49 for a review). An alternative for the hypothesis of de Gennes, which in some cases better captures experiments, is the "wetting hypothesis" of Ref. 50. In the latter description, randomness is not the deciding factor in the resulting phase behavior. However, it is clear that our simulations are only compatible with the random-field hypothesis of de Gennes, since we see large differences between randomly and non-randomly placed

obstacles.

Finally, having shown that domain formation in membranes with quenched obstacles belongs to the universality class of the 2D-RFIM, further insights might be gained by comparing to other systems in that class. The obvious candidates are filled polymer blends confined to thin films [51], for which the connection to the random-field Ising model was already noted [52]. Experiments have revealed that quenched filler particles dramatically limit phase separation dynamics [53]. Complete phase separation is typically not observed, but rather a mosaic of microscopic domains [54]. Computer simulations and theory [52, 55, 56] indicate that the dynamics can become completely arrested, leading to many "pinned" domains [57, 58]. Some of these results are in remarkable agreement with the membrane simulations of Refs. 18 and 19 and the present work.

ACKNOWLEDGMENTS

This work was supported by the *Deutsche Forschungsgemeinschaft* (Emmy Noether program: VI 483/1-1). We also acknowledge stimulating discussions at the CECAM workshop *Complex dynamics of fluids in disordered and crowded environments*, July 2010, where the results of this paper were first presented.

[1] S. J. Singer and G. L. Nicolson, *The fluid mosaic model of the structure of cell membranes.*, Science (New York, N.Y.) **175**, 720 (1972)

[2] P.-F. Lenne and A. Nicolas, *Physics puzzles on membrane domains posed by cell biology*, Soft Matter **5**, 2841 (2009)

[3] S. Veatch and S. Keller, *Seeing spots: Complex phase behavior in simple membranes*, Biochim. Biophys. Acta **1746**, 172 (2005)

[4] L. J. Pike, *The challenge of lipid rafts*, J. Lipid Res. **50**, 800040 (2008)

[5] K. Simons and E. Ikonen, *Functional rafts in cell membranes*, Nature **387**, 569 (1997)

[6] S. Ramachandran, M. Laradji, and P. B. S. Kumar, *Lateral Organization of Lipids in Multi-component Liposomes*, J. Phys. Soc. Jpn. **78**, 041006 (2009)

[7] M. Saxton, Current Topics in Membranes and Transport: Lateral Diffusion of Lipids and Proteins, vol. 48 of *Current Topics in Membranes and Transport*, chap. 8, 229–282 (Elsevier, 1999)

[8] G. Lenaz, *Lipid fluidity and membrane protein dynamics*, Biosci. Rep. **7**, 823 (1987)

[9] E. Castellana and P. Cremer, *Solid supported lipid bilayers: From biophysical studies to sensor design*, Surf. Sci. Rep. **61**, 429 (2006)

[10] T.-Y. Yoon, C. Jeong, S.-W. Lee, J. H. Kim, M. C. Choi, S.-J. Kim, M. W. Kim, and S.-D. Lee, *Topographic control of lipid-raft reconstitution in model membranes*, Nat. Mater. **5**, 281 (2006)

[11] A. R. Honerkamp-Smith, P. Cicuta, M. D. Collins, S. L. Veatch, M. den Nijs, M. Schick, and S. L. Keller, *Line Tensions, Correlation Lengths, and Critical Exponents in Lipid Membranes Near Critical Points*, Biophys. J. **95**, 236 (2008)

[12] S. L. Veatch, O. Soubias, S. L. Keller, and K. Gawrisch, *Critical fluctuations in domain-forming lipid mixtures*, PNAS **104**, 17650 (2007)

[13] A. Honerkamp-Smith, S. Veatch, and S. Keller, *An introduction to critical points for biophysicists; observations of compositional heterogeneity in lipid membranes*, Biochim. Biophys. Acta **1788**, 53 (2009)

[14] M. Fisher, *The theory of equilibrium critical phenomena*, Reports on Progress in Physics **30**, 615 (1967)

[15] A. Kusumi, C. Nakada, K. Ritchie, K. Murase, K. Suzuki, H. Murakoshi, R. S. Kasai, J. Kondo, and T. Fujiwara, *Paradigm shift of the plasma membrane concept from the two-dimensional continuum fluid to the partitioned fluid: high-speed single-molecule tracking of membrane molecules.*, Annu. Rev. Biophys. Biomol. Struct. **34**, 351 (2005)

[16] S. Goennenwein, M. Tanaka, B. Hu, L. Moroder, and E. Sackmann, *Functional Incorporation of Integrins into Solid Supported Membranes on Ultrathin Films of Cellulose: Impact on Adhesion*, Biophys. J. **85**, 646 (2003)

[17] W. G. Madden and E. D. Glandt, *Distribution functions for fluids in random media*, J. Stat. Phys. **51**, 537 (1988)

[18] A. Yethiraj and J. C. Weisshaar, *Why Are Lipid Rafts Not Observed In Vivo?*, Biophys. J. **93**, 3113 (2007)

[19] J. Gómez, F. Sagués, and R. Reigada, *Effect of integral proteins in the phase stability of a lipid bilayer: Application to raft formation in cell membranes*, J. Chem. Phys. **132**, 135104 (2010)

[20] A. King and D. Belanger, *Random-field effects in d = 2 and d = 3 ising systems*, Journal of Magnetism and Magnetic Materials **54-57**, 19 (1986)

[21] I. Morgenstern, K. Binder, and R. M. Hornreich, *Two-dimensional Ising model in random magnetic fields*, Phys. Rev. B **23**, 287 (1981)

[22] R. B. Stinchcombe, *Dilute Magnetism*, in: C. Domb and J. L. Lebowitz (Eds.), Phase Transitions and Critical Phenomena, vol. 7, 151 (Academic Press, London, 1983)

[23] N. G. Fytas, A. Malakis, and I. A. Hadjiagapiou, *Quenched bond randomness in marginal and non-marginal Ising spin models in 2D*, J. Stat. Mech. **2008**, 11009 (2008)

[24] G. Mazzeo and R. Kühn, *Critical behavior of the two-dimensional spin-diluted Ising model via the equilibrium ensemble approach*, Phys. Rev. E **60**, 3823 (1999)

[25] S. L. Veatch, P. Cicuta, P. Sengupta, A. Honerkamp-Smith, D. Holowka, and B. Baird, *Critical fluctuations in plasma membrane vesicles.*, ACS Chem. Biol. **3**, 287 (2008)

[26] B. Widom and J. S. Rowlinson, *New Model for the Study of Liquid-Vapor Phase Transitions*, J. Chem. Phys. **52**, 1670 (1970)

[27] S. L. Veatch, K. Gawrisch, and S. L. Keller, *Closed-Loop Miscibility Gap and Quantitative Tie-Lines in Ternary Membranes Containing Diphytanoyl PC*, Biophys J **90**, 4428 (2006)

[28] S. L. Veatch and S. L. Keller, *Separation of Liquid Phases in Giant Vesicles of Ternary Mixtures of Phospholipids and Cholesterol*, Biophys. J. **85**, 3074 (2003)

[29] T. Fischer and R. L. C. Vink, *The Widom-Rowlinson mixture on a sphere: elimination of exponential slowing down at first-order phase transitions*, J. Phys.: Condens. Matter **22**, 104123 (2010)

[30] K. Binder, *Applications of Monte Carlo methods to statistical physics*, Reports on Progress in Physics **60**, 487 (1997)

[31] K. Binder, *Finite size scaling analysis of ising model block distribution functions*, Z. Phys. B **43**, 119 (1981)

[32] K. Binder, *Critical Properties from Monte Carlo Coarse Graining and Renormalization*, Phys. Rev. Lett. **47**, 693 (1981)

[33] G. Orkoulas, M. E. Fisher, and A. Z. Panagiotopoulos, *Precise simulation of criticality in asymmetric fluids*, Phys. Rev. E **63**, 051507 (2001)

[34] S. Munro, *Lipid Rafts: Elusive or Illusive?*, Cell **115**, 377 (2003)

[35] D. Lingwood and K. Simons, *Lipid Rafts As a Membrane-Organizing Principle*, Science **327**, 46 (2010)

[36] B. Grossmann and M. L. Laursen, *The confined-deconfined interface tension in quenched QCD using the histogram method*, Nucl. Phys. B **408**, 637 (1993), key: grossmann.laursen:1993

[37] K. Binder, *Monte Carlo calculation of the surface tension for two- and three-dimensional lattice-gas models*, Phys. Rev. A **25**, 1699 (1982)

[38] J. Lee and J. M. Kosterlitz, *New numerical method to study phase transitions*, Phys. Rev. Lett. **65**, 137 (1990)

[39] A. Billoire, T. Neuhaus, and B. A. Berg, *A determination of interface free energies*, Nucl. Phys. B **413**, 795 (1994)

[40] K. Vollmayr, J. D. Reger, M. Scheucher, and K. Binder, *Finite size effects at thermally-driven first order phase transitions: A phenomenological theory of the order parameter distribution*, Zeitschrift für Physik B Condensed Matter **91**, 113 (1993)

[41] G. Johnson, H. Gould, J. Machta, and L. K. Chayes, *Monte Carlo Study of the Widom-Rowlinson Fluid Using Cluster Methods*, Phys. Rev. Lett. **79**, 2612 (1997)

[42] A. Aharony and A. B. Harris, *Absence of Self-Averaging and Universal Fluctuations in Random Systems near Critical Points*, Phys. Rev. Lett. **77**, 3700 (1996)

[43] G. Parisi and N. Sourlas, *Scale Invariance in Disordered Systems: The Example of the Random-Field Ising Model*, Phys. Rev. Lett. **89**, 257204 (2002)

[44] R. L. C. Vink, T. Fischer, and K. Binder, *Finite size scaling in Ising-like systems with quenched random fields: Evidence of hyperscaling violation*, arXiv:1008.3299 (2010)

[45] Y. Imry and S. K. Ma, *Random-Field Instability of the Ordered State of Continuous Symmetry*, Phys. Rev. Lett. **35**, 1399 (1975)

[46] L. Tamm and J. T. Groves, *Supported Membranes*, in: J. Struct. Biol., vol. 168, 1–222 (Elsevier, 2009)

[47] M. J. Saxton, *The spectrin network as a barrier to lateral diffusion in erythrocytes. A percolation analysis*, Biophys. J. **55**, 21 (1989)

[48] P. G. De Gennes, *Liquid-liquid demixing inside a rigid network: qualitative features*, J. Phys. Chem. **88**, 6469 (1984)

[49] R. L. C. Vink, *Critical behavior of soft matter fluids in bulk and in random porous media: from Ising to random-field Ising universality*, Soft Matter **5**, 4388 (2009)

[50] A. J. Liu, D. J. Durian, E. Herbolzheimer, and S. A. Safran, *Wetting transitions in a cylindrical pore*, Phys. Rev. Lett. **65**, 1897 (1990)

[51] Y. S. Lipatov, *Phase Separation in Filled Polymer Blends*, J. Macromol. Sci. Part B Phys. **45**, 871 (2006)

[52] M. Laradji and G. MacNevin, *Phase separation dynamics in binary fluids containing quenched or mobile filler particles*, J. Chem. Phys. **119**, 2275 (2003)

[53] H. Tanaka, A. J. Lovinger, and D. D. Davis, *Pattern evolution caused by dynamic coupling between wetting and phase separation in binary liquid mixture containing glass particles*, Phys. Rev. Lett. **72**, 2581 (1994)

[54] A. Karim, J. F. Douglas, G. Nisato, D.-W. Liu, and E. J. Amis, *Transient Target Patterns in Phase Separating Filled Polymer Blends*, Macromolecules **32**, 5917 (1999)

[55] F. Qiu, G. Peng, V. V. Ginzburg, A. C. Balazs, H. Y. Chen, and D. Jasnow, *Spinodal decomposition of a binary fluid with fixed impurities*, J. Chem. Phys. **115**, 3779 (2001)

[56] D. Suppa, O. Kuksenok, A. C. Balazs, and J. M. Yeomans, *Phase separation of a binary fluid in the presence of immobile particles: A lattice Boltzmann approach*, J. Chem. Phys. **116**, 6305 (2002)

[57] S. C. Glotzer, M. F. Gyure, F. Sciortino, A. Coniglio, and H. E. Stanley, *Pinning in phase-separating systems*, Phys. Rev. E **49**, 247 (1994)

[58] M. F. Gyure, S. T. Harrington, R. Strilka, and H. E. Stanley, *Scaling in late stage spinodal decomposition with quenched disorder*, Phys. Rev. E **52**, 4632 (1995)